Inducing Transport in a Dissipation-Free Lattice with Super Bloch Oscillations

Elmar Haller, Russell Hart, Manfred J. Mark, Johann G. Danzl, Lukas Reichsöllner, and Hanns-Christoph Nägerl

Institut für Experimentalphysik and Zentrum für Quantenphysik, Universität Innsbruck, Technikerstraße 25, 6020 Innsbruck, Austria

(Received 7 January 2010; revised manuscript received 11 March 2010; published 21 May 2010)

Particles in a perfect lattice potential perform Bloch oscillations when subject to a constant force, leading to localization and preventing conductivity. For a weakly interacting Bose-Einstein condensate of Cs atoms, we observe giant center-of-mass oscillations in position space with a displacement across hundreds of lattice sites when we add a periodic modulation to the force near the Bloch frequency. We study the dependence of these ''super'' Bloch oscillations on lattice depth, modulation amplitude, and modulation frequency and show that they provide a means to induce linear transport in a dissipation-free lattice.

DOI: 10.1103/PhysRevLett.104.200403 PACS numbers: 05.30.Jp, 03.75.Dg, 03.75.Lm, 67.85.−d

Understanding the conduction of electrons through solids is of fundamental concern within the physical sciences. The simplified situation of an electron under a constant force F within a perfect, nondissipative, periodic lattice was originally studied by Bloch and Zener [1] over 70 years ago. Their and subsequent studies revealed that the particle would undergo so-called Bloch oscillations (BOs), a periodic oscillation in position and momentum space, thereby quenching transport and hence resulting in zero conductivity. BOs can be viewed as periodic motion through the first Brillouin zone, resulting in a Bloch period $T_B = 2\hbar k/F$, where $k = \pi/d$ is the lattice wave vector for a lattice spacing d. They result from the interference of the particle's matter wave in the presence of the periodic lattice structure, requiring a coherent evolution of the wave during the time T_B. Generally, it is believed that conductance is restored via dissipative effects such as scattering from lattice defects or lattice phonons [2]. In bulk crystals, relaxation processes destroy the coherence of the system even before a single Bloch cycle is completed. These systems thus exhibit conductivity but prevent the observation of BOs. To observe BOs, the BO frequency $\nu_B = 1/T_B$ must be large compared to the rate of decoherence. In semiconductor superlattices, where the Bloch frequency is enhanced, a few cycles have been observed [3].

A recent approach to observe and study BOs is to use systems of ultracold atoms in optical lattice potentials with a force that is provided by gravity or by acceleration of the lattice potential. In these engineered potentials, generated by interfering laser waves, dissipation is essentially absent, and decoherence can be well controlled [4]. Essentially all relevant system parameters are tunable, e.g., lattice depth and spacing, particle interaction strength, and external force, i.e., lattice tilt. For sufficiently low temperatures, a well-defined narrow momentum distribution can initially be prepared. BOs have been observed for thermal samples [5–7], for atoms in weakly interacting Bose-Einstein condensates (BECs) [4,8,9], and for ensembles of noninteracting quantum-degenerate fermions [10]. Noninteracting BECs [11,12] are ideally suited to study BOs as interaction-induced dephasing effects are absent, allowing for the observation of more than 20 000 Bloch cycles [11].

As for any oscillator, classical or quantum, it is natural that one investigates the properties of the oscillator under forced harmonic driving. The dynamics of a harmonically driven Bloch oscillator has recently been the subject of several theoretical [13–16] and experimental studies [17–20]. For example, modulation-enhanced tunneling between lattice sites [18,19] and spatial breathing of incoherent atomic samples [20] have been observed. Here, for a weakly interacting atomic BEC in a tilted lattice potential, we demonstrate that harmonic driving can lead to directed center-of-mass motion and hence to transport. More strikingly, for slightly off-resonant driving, we observe giant matter-wave oscillations that extend over hundreds of lattice sites. These ''super-Bloch oscillations'' result from a beat between the usual BOs and the drive. They are rescaled BOs in position space and can also be used, by appropriate switching of the detuning or the phase, to engineer transport.

The experimental starting point is a tunable BEC of 1.2×10^5 Cs atoms in a crossed beam dipole trap [21] adiabatically loaded within 400 ms into a vertically oriented 1D optical lattice [11] as illustrated in Fig. 1(a). The lattice spacing is $d = \lambda/2$, where $\lambda = 1064.49(1)$ nm is the wavelength of the light. Unless stated otherwise, we work with a shallow lattice with depth $V = 3.0(3)E_R$, where $E_R = h^2/(2m\lambda^2)$ is the photon recoil energy for particles with mass m. The atoms are initially levitated against gravity by means of a magnetic field gradient and spread across approximately 50 lattice sites with an average density near 5×10^{13} cm^{-3} in the central region of the sample. We control the strength of the interaction as measured by the s-wave scattering length a near a Feshbach resonance [21]. Throughout this Letter, unless stated otherwise, we work at $a = 11(1)a_0$, where a_0 is Bohr's radius. We initiate BOs by removing the dipole trap confinement in the vertical direction and by reducing the levitation in 1 ms to cause a force that is a small fraction of the gravitational force mg, for which ν_B is near 100 Hz. An

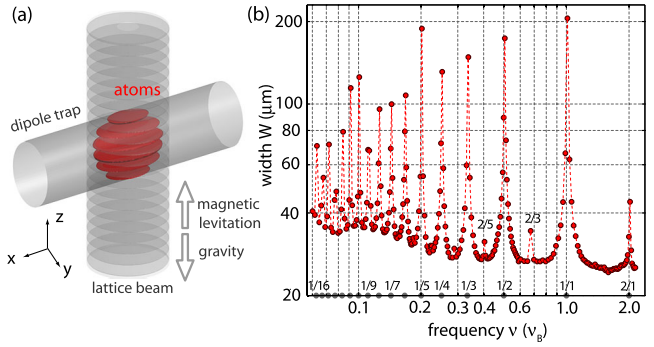

FIG. 1 (color online). Experimental setup (a) and excitation spectrum (b) for atoms in a tilted periodic potential. The width W is plotted as a function of the drive frequency ν. The resonances correspond to a drastic spreading of the atomic wave packet as a result of modulation-assisted tunneling [19] when $\nu \approx (i/j)\nu_B$, where i, j are integers. The parameters are $F_0 = 0.096(1)mg$, $\Delta F = 0.090(4)mg$, $V = 3.0(3)E_R$, and $\tau = 2$ s. The dashed line is a guide to the eye.

additional harmonic modulation of the levitation gradient then results in an oscillating driving force $F(t) = F_0 + \Delta F \sin(2\pi\nu t + \phi)$, where F_0 is the constant force offset, ΔF is the amplitude of the modulation, ν is the modulation frequency, and ϕ is a phase difference between the BOs and the drive. After a given hold time τ we switch off all optical beams and magnetic fields and take *in situ* absorption images after a short delay time of 800 μs.

We first determine the excitation spectrum. Figure 1(b) shows the $1/\sqrt{e}$ width W of the matter wave after $\tau = 2$ s as a function of ν. A series of narrow resonances at rational multiples of ν_B can clearly be identified. In agreement with recent experiments [18,19], we attribute these resonances to modulation-enhanced tunneling between lattice sites, leading to dramatic spreading of the atomic wave packet. Tunneling between nearest neighbor lattice sites is enhanced when ν_B is an integer multiple j of ν via a j-phonon process [22], while tunneling between lattice sites i lattice units apart is enhanced when ν is an integer multiple i of ν_B. Even combinations thereof, e.g., $i/j = 2/3$ or $2/5$, are detectable.

We now investigate the dynamics of the wave packet in more detail. For this, we use the resonance with $i = j = 1$ and choose $\nu = \nu_B + \Delta\nu$, where $\Delta\nu$ is the detuning. In Figs. 2(a)–2(d) we present absorption images and spatial profiles for the weakly interacting BEC. The time evolution for the width, shape, and center position of the BEC is dramatic. On resonance ($\Delta\nu = 0$), (c) and (d), the atomic ensemble spreads as it develops pronounced edges. Also, as we will see below, the center-of-mass motion depends crucially on the phase ϕ. Off resonance, (a) and (b), for small detuning $\Delta\nu = -1$ Hz, the wave packet exhibits giant oscillatory motion across hundreds of lattice sites that we denote as "super Bloch oscillations" (SBO). Note that, for the parameters used here, the amplitude for ordinary BOs corresponds to about $4d = 2.1$ μm. Also the width and higher moments of the distribution show oscillatory behavior. In Fig. 2(e) we plot the center-of-mass position as a function of time for $\Delta\nu = -1$ Hz. At $a = 11(1)a_0$ we typically observe SBOs over the course of several seconds. The dynamics of SBOs strongly depends upon the site-to-site phase evolution of the matter wave. In fact, stronger interactions, e.g., $a = 90(1)a_0$, distort the density profile of the driven BEC and alter the BEC's oscillation frequency and amplitude. For sufficiently strong interactions, no SBOs are observed. We also attribute the wave-packet spreading as seen after one cycle in Fig. 2(b) mostly to interactions. For the measurements above, we intentionally use a large modulation amplitude ΔF to enhance the amplitude of SBOs. However, all effects equally exist for $\Delta F \ll F_0$, as we will also demonstrate below in Fig. 4(b).

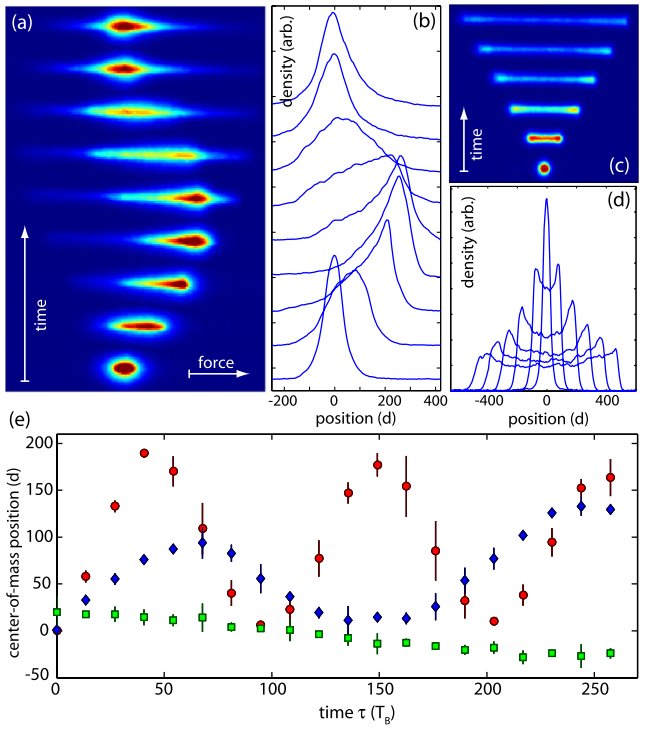

FIG. 2 (color online). Observation of super-Bloch oscillations and modulation-driven wave-packet spreading. (a) and (b) *In situ* absorption images and density profiles for off-resonant modulation ($\Delta\nu = -1$ Hz), showing giant oscillatory motion across more that 200 sites. (time steps of 120 ms, average of 4 images). (c) and (d) *In situ* absorption images and density profiles for resonant modulation ($\Delta\nu = 0$ Hz), showing a wave packet that spreads symmetrically (time steps of 100 ms, average of 4 images). The phase ϕ was adjusted to allow for a symmetric spreading, corresponding to a calculated value of $\phi = \pi/2$. For (a)–(d), the parameters are $F_0 = 0.062(1)mg$, $\Delta F = 0.092(4)mg$, $V = 3.0(3)E_R$, $a = 11(1)a_0$. (e) Center-of-mass motion for $a = 11(1)a_0$ (circles), $a = 90(1)a_0$ (diamonds), $a = 336(4)a_0$ (squares).

It is useful to develop a simple semiclassical model to obtain a qualitative understanding of the origin of SBOs. The only elements of this model are that the wave packet is accelerated by the applied force and that, once the wave

packet reaches the edge of the first Brillouin zone, it is Bragg reflected. This model does not include an effective mass and cannot be used to predict quantitative results. Figures 3(a)–3(d) show the result of a numerical integration of the time-dependent acceleration $a(t) = F_0/m + \Delta F/m \sin[2\pi(\nu_B + \Delta\nu)t + \phi]$ with periodic Bragg reflection. For a constant acceleration $\Delta F = 0$, the wave packet's velocity shows the well-known saw-tooth-like time evolution that corresponds to BOs. The curve in (a) is symmetric, hence, there is no net movement, as indicated by the shaded regions of equal area. If, however, there is additional harmonic modulation at $\nu = \nu_B$, the velocity excursions will not be symmetric about zero, (b), and result in a net movement for each period, leading to linear motion, (c). Only for $\phi = \pi/2$ or $\phi = 3\pi/2$ symmetry is restored and no net movement will occur. Note that, in general, the velocity of the linear motion depends nontrivially on ϕ. Off-resonant modulation with $\Delta\nu \ll \nu_B$ induces a slowly varying phase mismatch between the drive and the original Bloch period. This results in a slow oscillation of the net movement for each Bloch cycle, which finally sums up to a giant oscillation in position space, (d). Evidently, this oscillation is the result of a beat between the drive and the original BO. The initial direction of the motion depends on ϕ and $\Delta\nu$. In particular, a change in the sign of $\Delta\nu$ at a given ϕ can lead to opposite motion in position space, as verified experimentally in Fig. 3(e) for $\Delta\nu = \pm 1$ Hz.

A quantitative understanding of SBOs [16] can be obtained from an approach based on Wannier-Stark states [15]. In essence, the harmonic drive is expected to lead to a rescaling of the tunneling rate $J \rightarrow J_{\mathrm{eff}} = JB_1(\Delta F/F_0)$ and the force $F_0 \rightarrow F_{\mathrm{eff}} = h\Delta\nu/d$ for a stationary lattice with tilt. Here, B_1 is the first Bessel function of the first kind. The amplitude of SBOs is thus given by a new Wannier-Stark localization length $L_{\mathrm{eff}} \approx J_{\mathrm{eff}}/(dF_{\mathrm{eff}})$ [16]. In this sense, SBOs are rescaled BOs. We quantitatively study the dependence of amplitude and period of SBOs on $\Delta\nu$, $\Delta F/F_0$, and V. The results are shown in Fig. 4. As expected, the period T is given by $1/\Delta\nu$. Also, the oscillation amplitude scales as $1/\Delta\nu$, and its Bessel-function dependence on $\Delta F/F_0$ is well reproduced. Given our spatial resolution, we can observe SBOs down to $\Delta F/F_0 = 0.08$ [Fig. 4(b)]. Note that SBOs can only be observed with sufficient wave function coherence and for

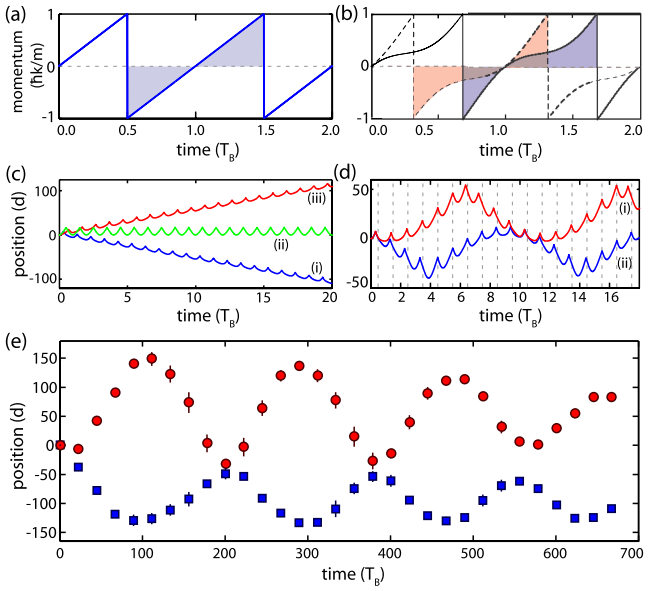

FIG. 3 (color online). Results from a semiclassical model for SBOs. (a) For a constant force, here $F_0 = 0.06mg$, the velocity (in units of $\hbar k/m$) exhibits a symmetric, saw-tooth-like time evolution, typical for BOs. (b) Resonant modulation, here with $\Delta F = 0.8F_0$, alters the symmetric periodic velocity excursions of normal BOs ($\phi = 0$, solid line, $\phi = \pi$, dashed line), leading to a net movement, (c), with $\phi = 0$ (i), $\phi = \pi/2$ (ii), and $\phi = \pi$ (iii). An additional detuning $\Delta\nu = \pm 0.1\nu_B$ results in a periodically changing phase difference and hence in giant oscillations in position space, (i) and (ii) in (d). On top of the motion, normal BOs can clearly be seen. The phase of SBOs depends on the sign of $\Delta\nu$, as shown by experimental data in (e), where $F_0 = 0.096(1)mg$, $\Delta F = 0.090(4)mg$, $\Delta\nu = 1$ Hz (circles), -1 Hz (squares).

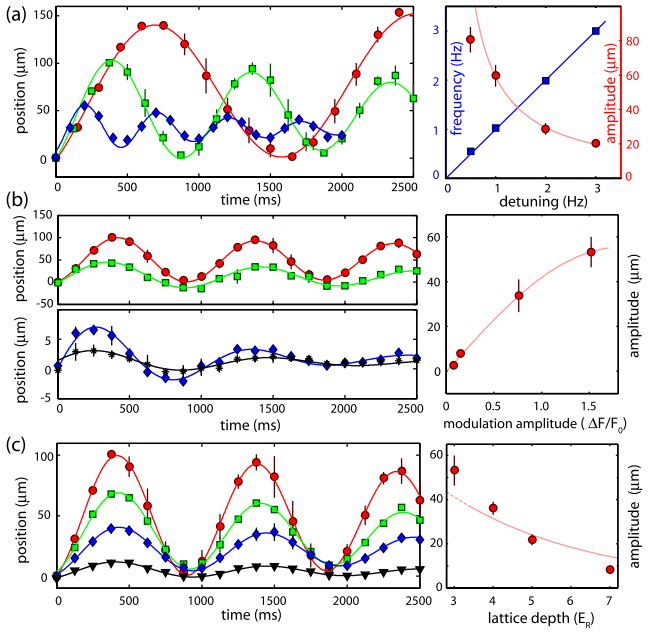

FIG. 4 (color online). Quantitative analysis of SBOs. (a) The effect of the detuning $\Delta\nu$ on the oscillation frequency and the amplitude of SBOs, with $\Delta\nu = 0.5$ Hz (circles), 1 Hz (squares), 2 Hz (diamonds). Right: The solid lines are fits with linear and $\Delta\nu^{-1}$ dependence, respectively. (b) Dependence of the amplitude of SBOs on $\Delta F/F_0$. The data sets correspond to $\Delta F/F_0 =$ 1.52 (circles), 0.76 (squares), 0.15 (diamonds), 0.08 (stars). Right: The solid line is a fit proportional to $B_1(\Delta F/F_0)$. (c) Amplitude of SBOs as a function of lattice depth, $V = 3E_R$ (circles), $4E_R$ (squares), $5E_R$ (diamonds), $7E_R$ (triangles). Right: The solid line is a fit proportional to J, for which we omit the first data point for the shallow lattice. If not stated otherwise, the parameters for all measurements shown here are $F_0 = 0.062(1)mg$, $\Delta F = 0.092(4)mg$, $\Delta\nu = -1$ Hz.

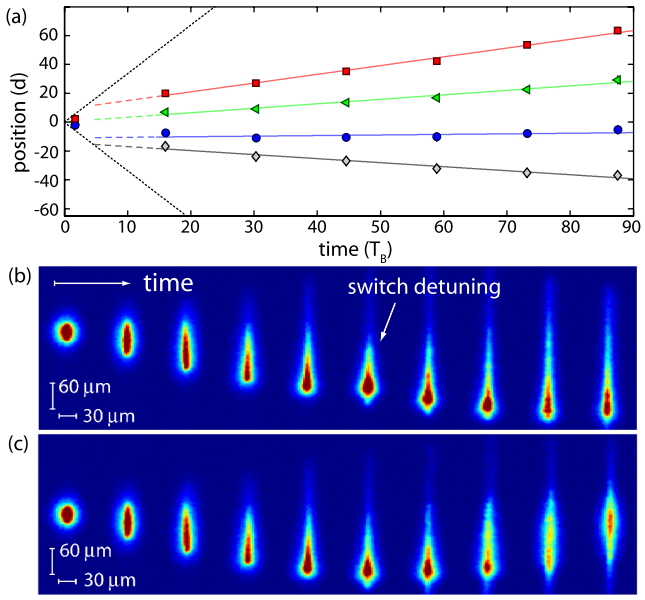

FIG. 5 (color online). Inducing transport. (a) Linear motion for resonant modulation. $\Delta\phi = 0°$ diamonds, 65° circles, 120° triangles, 190° squares. $\Delta\phi = 0°$ and $\Delta\phi = 190°$ were chosen to maximize the speed in opposite directions. The solid lines are linear fits to the data points excluding the first data point. For comparison we plot the linear motion that corresponds to a tunneling rate of J_{eff}, dotted lines. (b) Directed motion for off-resonant modulation. $\Delta\nu$ was switched from -1 to 1 Hz after 400 ms. For comparison, (c) shows the oscillatory motion without switching (time steps of 80 ms). The parameters are $F_0 = 0.096(1)mg$, $\Delta F = 0.090(4)mg$.

well-defined initial conditions, i.e., for sufficient wave-packet localization in the first Brillouin zone of the lattice. Nevertheless, incoherent atomic samples exhibit a breathing of the spatial distribution [20] as the oscillation period is insensitive to the initial conditions. In the work of Ref. [20], the breathing can be understood in terms of an incoherent sum over localized Wannier-Stark states that individually show a breathing motion with period T [15].

The results above provide two mechanisms to circumvent the localization inherent in BOs and to induce coherent transport in an otherwise insulating context. As shown in Fig. 5(a), resonant modulation ($\Delta\nu = 0$) causes directed motion of the wave packet's center of mass. For longer times, we find that the motion is approximately linear. The mean velocity depends on the relative phase ϕ of the Bloch oscillator and the drive. In the experiment, we varied ϕ via $\phi = \phi_0 + \Delta\phi$, where ϕ_0 is a constant phase offset, which depends on the details how BOs are initiated. For off-resonant modulation, transport can be induced by switching the sign of $\Delta\nu$ before a half-cycle of a SBO is completed. The wave-packet then continues to move in the original direction. This motion is shown in Fig. 5(b), where we switch the sign after 400 ms. For comparison, Fig. 5(c) shows a SBO with $T = 1$ s without switching.

In summary, we have studied the coherent evolution of matter waves in tilted periodic potentials under forced driving and have observed giant SBOs, which result from a beat of BOs with the drive when a small detuning $\Delta\nu$ from the Bloch frequency is introduced. Localization as a result of BOs is broken, allowing us to engineer matter-wave transport over macroscopic distances in lattice potentials with high relevance to atom interferometry [23]. We are now in a position to investigate the effect of interactions on driven transport, for which subdiffusive and chaotic dynamics have been proposed [24].

We thank A. R. Kolovsky, A. Zenesini, and A. Wacker for discussions and R. Grimm for generous support. We acknowledge funding by the Austrian Ministry of Science and Research and the Austrian Science Fund and by the European Union within the framework of the EuroQUASAR collective research project QuDeGPM. R. H. is supported by a Marie Curie Action within FP7.

Note added.—Recently, we became aware of related work on nondissipative transport in a quantum ratchet [25].

[1] F. Bloch, Z. Phys. **52**, 555 (1929); C. Zener, Proc. R. Soc. A **145**, 523 (1934).
[2] Y. Kanemitsu and T. Ogawa, *Optical Properties of Low-Dimensional Materials* (World Scientific, Singapore, 1995); N. W. Ashcroft and N. D. Mermin, *Solid State Physics* (Saunders College, Philadelphia, 1976).
[3] K. Leo *et al.*, Solid State Commun. **84**, 943 (1992); J. Feldmann *et al.*, Phys. Rev. B **46**, 7252 (1992).
[4] M. Gustavsson *et al.*, arXiv:0812.4836.
[5] M. Ben Dahan *et al.*, Phys. Rev. Lett. **76**, 4508 (1996).
[6] R. Battesti *et al.*, Phys. Rev. Lett. **92**, 253001 (2004).
[7] G. Ferrari *et al.*, Phys. Rev. Lett. **97**, 060402 (2006).
[8] B. P. Anderson and M. A. Kasevich, Science **282**, 1686 (1998).
[9] O. Morsch *et al.*, Phys. Rev. Lett. **87**, 140402 (2001).
[10] G. Roati *et al.*, Phys. Rev. Lett. **92**, 230402 (2004).
[11] M. Gustavsson *et al.*, Phys. Rev. Lett. **100**, 080404 (2008).
[12] M. Fattori *et al.*, Phys. Rev. Lett. **100**, 080405 (2008).
[13] H. J. Korsch and S. Mossmann, Phys. Lett. A **317**, 54 (2003).
[14] T. Hartmann *et al.*, New J. Phys. **6**, 2 (2004).
[15] Q. Thommen, J. C. Garreau, and V. Zehnlé, Phys. Rev. A **65**, 053406 (2002); J. Opt. B **6**, 301 (2004).
[16] A. Kolovsky and H. J. Korsch, arXiv:0912.2587.
[17] S. R. Wilkinson *et al.*, Phys. Rev. Lett. **76**, 4512 (1996).
[18] V. V. Ivanov *et al.*, Phys. Rev. Lett. **100**, 043602 (2008).
[19] C. Sias *et al.*, Phys. Rev. Lett. **100**, 040404 (2008).
[20] A. Alberti *et al.*, Nature Phys. **5**, 547 (2009).
[21] T. Kraemer *et al.*, Appl. Phys. B **79**, 1013 (2004).
[22] A. Eckardt *et al.*, Phys. Rev. Lett. **95**, 200401 (2005).
[23] A. D. Cronin, J. Schmiedmayer, and D. E. Pritchard, Rev. Mod. Phys. **81**, 1051 (2009).
[24] A. R. Kolovsky, E. A. Gómez, and H. J. Korsch, arXiv:0904.4549.
[25] T. Salger *et al.*, Science **326**, 1241 (2009).